Frontiers in Bioscience Landmark

Front. Biosci. (Landmark Ed) **2025**; 30(7): 40363
https://doi.org/10.31083/FBL40363

Original Research

Na^+,-K^+-ATPase Deficiency Exacerbates Cardiac Fibrosis via Promoting ERRα-Mediated Myocardial Cell Injury and Macrophage Activation Under Isoproterenol-Challenged Conditions

Ting Lei[1], Tao Liu[1,2], Yutong Liu[2], Yingnan Zhai[2], Ruijia Wang[2], Xiaoyi Tan[2], Hongli Liu[1,*], Xiaofei Yan[2,*]

[1]Department of Clinical Laboratory, Xi'an People's Hospital (Xi'an Fourth Hospital), 710004 Xi'an, Shaanxi, China
[2]Department of Biochemistry and Molecular Biology, Xi'an Jiaotong University, 710061 Xi'an, Shaanxi, China
*Correspondence: liuhongli@mail.xjtu.edu.cn (Hongli Liu); 279057894@qq.com (Xiaofei Yan)
Academic Editor: Ioanna-Katerina Aggeli
Submitted: 7 May 2025 Revised: 17 June 2025 Accepted: 24 June 2025 Published: 29 July 2025

Abstract

Background: Inflammation plays a pivotal role in the progression of tissue fibrosis. Our previous research demonstrated that Na^+, K^+-ATPase (NKA) α1 deficiency impairs mitochondrial function and accelerates isoproterenol (ISO)-induced cardiac remodeling. This study aims to investigate the interplay between inflammation and NKAα1 deficiency in ISO-induced cardiac fibrosis. **Methods**: Age-matched male wild-type (WT) and NKA$\alpha1^{+/-}$ mice received daily subcutaneous injections of ISO (30 mg/kg body weight) over 14 consecutive days. Comprehensive histopathological evaluation was performed to assess myocardial architecture and leukocyte infiltration profiles. Mitochondrial ultrastructure was analyzed using transmission electron microscopy. The molecular techniques of real-time quantitative polymerase chain reaction (RT-qPCR), immunoblotting, and enzyme-linked immunosorbent assay (ELISA) were utilized to quantify fibrotic markers and inflammatory mediators. A cell co-culture model was established to investigate the interactions between different cell types. **Results**: NKAα1 haploinsufficiency exacerbated heart lesions and fibrosis, led to macrophage accumulation, and increased the expression of inflammatory factors in ISO-challenged hearts. Although NKAα1 deficiency did not directly activate macrophages or fibroblasts under ISO conditions, it significantly accelerated cardiomyocyte death in response to ISO insult. Paracrine crosstalk between damaged NKA$\alpha1^{+/-}$ cardiomyocytes, macrophages, and fibroblasts amplified macrophage activation, inflammatory cytokine release, and fibroblast differentiation. Estrogen-related receptor α (ERRα) was identified as a key mediator of NKAα1 haploinsufficiency-induced cardiomyocyte death and interleukin-18 (IL-18) release. Furthermore, treatment with an NKAα1 ^{897}DVEDSYGQQWTYEQR^{911} (DR)-region antibody mitigated ISO-induced cardiac fibrosis and macrophage infiltration. **Conclusion**: This study provides evidence that NKAα1 deficiency exacerbates cardiac fibrosis by promoting ERRα-dependent cardiomyocyte death and by facilitating intercellular cross-talk between damaged NKA$\alpha1^{+/-}$ cardiomyocytes, macrophages, and fibroblasts. Based on these findings, we suggest that NKAα1 may be a potential regulator of cardiac fibrosis, and that its DR-region represents a potential therapeutic target.

Keywords: fibrosis; isoproterenol; inflammation; macrophages; mitochondria; NKA

1. Introduction

Heart fibrosis is a maladaptive remodeling process characterized by excessive deposition of extracellular matrix (ECM) proteins and collagen fibers in the cardiac interstitium [1]. While cardiac fibrosis initially serves as a compensatory mechanism to uphold tissue architecture and physiological stability following myocardial injury, this process progressively diminishes myocardial elasticity and impairs cardiac conduction, culminating in disease-related morbidity and mortality [2]. Although regression of fibrotic myocardium occurs sporadically, development of precision-targeted treatments remains largely elusive [3]. Identifying novel therapeutic targets driving cardiac fibrosis remains an urgent priority in cardiovascular research.

Dysregulated inflammation plays a critical role in heart fibrosis [4]. For instance, studies in small animal models have demonstrated that macrophages can drive heart fibrotic remodeling and ventricular dysfunction, while T cells coordinate fibrosis in non-ischemic heart failure [5,6]. During the progression of various forms of heart failure, cardiomyocyte death, fibroblast activation, and inflammatory cytokine release are interconnected processes that exacerbate tissue fibrosis [7].

Na^+, K^+-ATPase (NKA) serves as a classical ion pump that spans the cell membrane and actively transports Na^+ out of and K^+ into the cell, thereby maintaining membrane potential [8]. Besides its canonical ion-pumping role, NKA also functions as a signaling transducer, modulating Src signaling cascades, the PI3K/AKT pathway, P2X7R/K^+ cascades, and cytosolic Ca^{2+} oscillations [9,10]. Mature cardiomyocytes predominantly express the α1 isoform, accounting for approximately 75% of total NKAα subunit expression [11]. In the heart, NKA

Copyright: © 2025 The Author(s). Published by IMR Press.
This is an open access article under the CC BY 4.0 license.

Publisher's Note: IMR Press stays neutral with regard to jurisdictional claims in published maps and institutional affiliations.

performs vital physiological functions. A clinical studies have reported reduced NKA levels in left ventricular biopsies of dilated cardiomyopathy (DCM) subjects [12]. An animal study further indicated that administration of marinobufagenin, a natural NKA inhibitor, stimulated fibroblast collagen production and induces cardiac fibrosis [13]. Previously, we observed that NKA deficiency impairs mitochondrial function, accelerating isoproterenol (ISO)-induced cardiac fibrosis and dysfunction [14]. However, whether inflammation contributes to NKA deficiency-related cardiac fibrosis remains unclear. Herein, we aim to elucidate the relationship between inflammation and cardiac fibrosis under NKA-deficient conditions.

2. Materials and Methods

2.1 Chemicals and Antibodies

All compounds, including ISO (Cat No. 420355) and SLU-PP-332 (Cat No. SML3908), were commercially sourced from Sigma-Aldrich (St. Louis, MO, USA). Mouse IgG was sourced from Bioss Biotechnology Company (Beijing, China, Cat No. bs-0296P). DRm217 antibody, a particular antibody targeting the DR-region (^{897}DVEDSYGQQWTYEQR^{911}) of the NKAα1 subunit, was prepared in our lab [15]. The primary antibodies against α-smooth muscle actin (α-SMA, Cat No. GB111364-50), CD68 (Cat No. GB113109-50), LY6G (Cat No. GB11229-50), CD3 (Cat No. GB13014-50), and Horseradish Peroxidase (HRP)-labeled rabbit antibodies (Cat No. GB23303) were sourced from Servicebio Technology Company (Wuhan, Hubei, China). Primary antibody targeting estrogen-related receptor α (ERRα, Cat No. CY5617) was sourced from Abways company (Shanghai, China), and primary antibody targeting β-actin (Cat No. 66009-1-Ig) was sourced from Proteintech Biotechnology Company (Wuhan, Hubei, China).

2.2 Animal Model Establishment

All animal procedures were approved by the Animal Care and Use Committee of Xi'an Jiaotong University (Ethics numbers: IAUC/765/2019, #19765) and adhered to guidelines established by the National Health and Medical Research Council of China. Eight-week-old male wild-type (WT) and NKA$\alpha1^{+/-}$ mice were subcutaneously injected with ISO (30 mg/kg) daily for 14 consecutive days. Following euthanasia via cervical dislocation, hearts were harvested for subsequent analyses. To evaluate the effects of DRm217, 18 male C57BL/6 mice were randomly assigned to saline, ISO+IgG, or ISO+DRm217 groups. IgG or DRm217 was administered intraperitoneally at a dose of 10 mg/kg every 5 days.

2.3 Histological Analysis

To evaluate histopathological changes, the hearts were rinsed with 0.9% saline and subsequently fixed in 4% paraformaldehyde. Each heart was divided into three segments and embedded in paraffin. Serial sections of 5 µm thickness were prepared from the basal, mid, and apical levels of the heart. The sections were stained with hematoxylin and eosin (H&E). A pathologist who was blinded to the identify of experimental groups evaluated the histopathological scores based on hyper-eosinophilic bundles, leukocyte infiltration, and cardiomyocyte necrosis. At least 10 fields per slide were examined, with the severity of changes graded as severe (++++), moderate (+++), mild (++), minimal (+), or nil (–). The extent of myocardial fibrosis was assessed using Masson's trichrome staining, while collagen content was quantified after staining with Sirius red. Histopathological images were captured and analyzed using a digital camera attached to a microscope (Nikon, Tokyo, Japan). The percentage of fibrotic area in each image was measured using ImageJ software (VERSION 1.53t, National Institutes of Health, Bethesda, MD, USA), and calculated as the ratio of positively stained areas to the total field area.

2.4 Immunohistochemical Staining

For antigen retrieval, paraffin-embedded sections were deparaffinized, rehydrated, and immersed in 0.01 M citric acid buffer (pH 10.0). Sections were treated with 3% hydrogen peroxide for 10 minutes to quench endogenous peroxidase activity, then blocked with rabbit serum for 30 minutes at room temperature. Subsequently, the slides were incubated overnight at 4 °C with primary antibodies against CD68 (1:100), Ly6G (1:100), CD3 (1:100), or α-SMA (1:100). Next, slides were incubated with HRP-labeled goat anti-rabbit secondary antibody for 1 h. Sections were then washed, stained with 3,3'-Diaminobenzidine (DAB) (Cat No. G1212-200T, Servicebio Technology Company, Wuhan, Hubei, China), and counterstained with hematoxylin. Histopathological images were captured and analyzed using a digital camera linked to a microscope (Nikon, Tokyo, Japan). To quantify immunohistochemistry results, a pathologist blinded to the experimental groups counted cells with positive immunostaining for CD68, Ly6G, and CD3. For alpha-smooth muscle actin (α-SMA) staining, the positively stained area was analyzed using ImageJ software and expressed as the percentage of stained cortical area relative to the total area.

2.5 Western Blotting

Heart tissues were homogenized in RIPA lysis buffer containing a protease inhibitor cocktail (Roche, Basel, Switzerland) and a phosphatase inhibitor cocktail (Sigma, St. Louis, MO, USA). After incubation on ice for 30 minutes, the supernatant was collected by centrifugation for 20 minutes at 4 °C and 12,000 rpm. Protein samples were separated by 10% Sodium Dodecyl Sulfate–Polyacrylamide Gel Electrophoresis (SDS-PAGE) and transferred onto a Polyvinylidene Fluoride (PVDF) membrane (Thermo Fisher Scientific, Waltham, MA, USA). The membrane

was blocked with 10% milk in TBST buffer (10 mM Tris-HCl, 120 mM NaCl, and 0.1% Tween 20, pH 7.4) for 1 h at room temperature and then incubated with ERRα primary antibody (1:1000) overnight at 4 °C. Membranes were washed three times with TBST buffer and incubated with horseradish peroxidase-conjugated anti-rabbit IgG (1:5000) for 1 h at room temperature. After washing, visualization was performed using an enhanced chemiluminescence kit (GE Healthcare, Chicago, IL, USA). Protein bands were captured using ImageQuant LAS 400 (GE Healthcare, Chicago, IL, USA) and band intensity was quantified by densitometry analysis using ImageJ (version 1.53t, National Institutes of Health, Bethesda, MD, USA).

2.6 Transmission Electron Microscopy

Cardiac tissues were fixed in 3% glutaraldehyde for 24 h and subsequently fixed in 1% osmium tetroxide for 1 h. Following dehydration in an ethanol gradient and 2% uranyl acetate staining, samples were embedded in Embed 812 resin for transmission electron microscopy (JEM-1400PLUS, JEOL, Tokyo, Japan) ultrastructural assessment. The images were reviewed in a blinded fashion by two radiologists.

2.7 Enzyme-Linked Immunosorbent Assay (ELISA)

The levels of interleukin-6 (IL-6, BGK08505), tumor necrosis factor-α (TNF-α, BGK06804), interleukin-1β (IL-1β, BGK10749), and interleukin-18 (IL-18, ab216165) were measured using corresponding ELISA kits (Peprotech Company, Rocky Hill, NJ, USA for IL-6, TNF-α, and IL-1β, and Abcam Company, Shanghai, China for IL-18) according to the manufacturer's instructions.

2.8 Cell Isolation and Treatment

Ventricular cardiomyocytes, macrophages, and fibroblasts were isolated from WT or NKA$\alpha 1^{+/-}$ mice as previously described [16]. Cardiomyocytes were identified based on their characteristic rod-shaped morphology under light microscopy. Fibroblasts were recognized by their characteristic spindle-shaped or stellate morphology with cytoplasmic processes, along with relatively large oval-to-fusiform nuclei, observed under microscopy. Macrophages were confirmed using flow cytometry with antibodies against F4/80. To ensure uniformity across treatments and comparisons, isolation of cardiomyocytes, fibroblasts, and macrophages followed a strictly standardized protocol performed consistently by the same technician for all groups. Isolated cardiomyocytes were cultured on 0.1% gelatin-precoated 6-well plates in Minimum Essential Medium (MEM, Thermo Fisher Scientific, Waltham, MA, USA, Cat No. 11095080) supplemented with 5% fetal bovine serum (FBS, Lonsa Science SRL, Suzhou, China, Cat No, S711-050S), 100 U/mL penicillin (Thermo Fisher Scientific, Waltham, MA, USA, Cat No. 15070063), and 100 mg/mL streptomycin (Thermo Fisher Scientific, Waltham, MA, USA, Cat No. 15070063). Isolated macrophages were quantified and seeded in RPMI-1640 (Thermo Fisher Scientific, Waltham, MA, USA, Cat No. 11875093) medium supplemented with 10% FBS, 100 mg/mL streptomycin, and 100 U/mL penicillin. Isolated fibroblasts were quantified and seeded in DMEM (Thermo Fisher Scientific, Waltham, MA, USA, Cat No. 11965092). The isolated ventricular cardiomyocytes, macrophages, and fibroblast have undergone mycoplasma infection testing. To detect the effects of ISO on cardiomyocytes, macrophages and fibroblasts, 10 µM ISO was added to the culture medium for 48 h. For DRm217 treatment, IgG or DRm217 was suppled 15 minutes after ISO addition at a final dose of 1 µM concentration. To detect the effects of SLU-PP-332, a specific ERR agonist, it was suppled in cell culture medium at a final dose of 1 µM concentration.

2.9 Cell Co-Culture

For the co-culture models of cardiomyocytes with macrophages or fibroblasts, cardiomyocytes were pre-plated in 6-well plates at a density of 5×10^5 cells/mL. Macrophages or fibroblasts were seeded onto cell culture inserts at a density of 1.0×10^5 cells/cm^2. The inserts containing macrophages or fibroblasts were then placed above the wells containing cardiomyocytes. These cells were co-cultured in MEM supplemented with 10 µM ISO or vehicle for 48 h. For the co-culture model of macrophages and fibroblasts, fibroblasts were pre-plated in 6-well plates at a density of 5×10^5 cells/mL. Inserts containing previously activated macrophages were placed above the wells containing fibroblasts. These cells were co-cultured in DMEM medium for 48 h.

2.10 Detection of Lactate Dehydrogenase (LDH) Activity

Cellular injury was assessed by measuring LDH release. Following 48 h treatment with ISO (10 µM), LDH activity in the culture medium was measured using a Roche LDH assay kit (Cat No. 04744926001, Mannheim, Germany) according to the manufacturer's protocol and a microplate reader.

2.11 Real-Time Quantitative PCR

Total RNA was isolated from heart tissue and cells using Trizol reagent (Cat No. B610409-0100, Sangon, Shanghai, China) and reverse-transcribed into cDNA using the MightyScript™ RT reagent kit (Cat No. B639252, Sangon, Shanghai, China). Quantitative polymerase chain reaction (qPCR) was performed using the SYBR Green reagent kit (Cat No. B532955, Sangon, Shanghai, China) on a QuantStudio™ 3 Real-Time PCR System (Bio-Rad, Hercules, CA, USA). Primer sequences used for qRT-PCR are listed in Table 1. All amplifications were normalized to β-actin. Data were analyzed using the comparative Ct ($2^{-\Delta\Delta Ct}$) method and expressed as fold change relative to the respective control.

Table 1. Primer sequences used for real-time quantitative PCR.

Gene	Species	Forward primer	Reverse primer
Acta2	Mouse	GTCCCAGACATCAGGGAGTAA	TCGGATACTTCAGCGTCAGGA
Fn1	Mouse	GATGCACCGATTGTCAACAG	TGATCAGCATGGACCACTTC
Col3a1	Mouse	TGACTGTCCCACGTAAGCAC	GGAGGGCCATAGCTGAACTG
Col1a1	Mouse	CGCAAAGAGTCTACATGTCTAGG	CATTGTGTATGCAGCTGACTTC
β-actin	Mouse	TGCTGTCCCTGTATGCCTCTG	TGATGTCACGCACGATTTCC

PCR, polymerase chain reaction; *Acta2*, actin alpha 2, smooth muscle, also named alpha-smooth muscle actin; *Fn1*, fibronectin 1; *Col3a1*, Collagen, type III, alpha 1; *Col1a1*, Collagen, type I, alpha 1; *β-actin*, beta-actin.

2.12 Statistical Analysis

Data are presented as the mean ± standard error. Statistical analysis was performed using SPSS software (version 22.0; IBM Corporation, Armonk, NY, USA). Student's *t*-test was used for comparisons between two groups. Multiple group comparisons were analyzed by one-way ANOVA followed by Tukey's post hoc test. A p-value < 0.05 was considered statistically significant.

3. Results

3.1 NKAα1 Insufficiency Aggravats ISO-Induced Cardiac Lesion and Fibrosis

Since animals completely lacking the α1 gene suffer from embryonic lethality, heterozygous mice lacking only one copy of the allele ($\alpha1^{+/-}$) are a commonly used experimental model. H&E staining revealed myocardial cell rupture, cellular vacuolization, and inflammatory cell infiltration in WT mice treated with ISO. These pathological alterations were more pronounced in NKA$\alpha1^{+/-}$ mice treated with ISO (Fig. 1A,B). NKAα1 haploinsufficiency also increased interstitial collagen deposition under ISO treatment, as evidenced by Masson trichrome staining and Sirius red staining (28.13 ± 2.54% vs. 8.72 ± 1.26% for Masson staining; 28.46 ± 2.24% vs. 9.61 ± 1.15% for Sirius red staining, $p < 0.05$) (Fig. 1C,D). These results demonstrate that NKAα1 haploinsufficiency exacerbates heart lesions and fibrosis under ISO challenge.

3.2 NKAα1 Haploinsufficiency Led to Aberrant ECM Protein Deposition and Myofibroblast Differentiation

Our previous unbiased proteomic analysis of cardiac tissues from WT and NKA$\alpha1^{+/-}$ mice challenged with ISO revealed differential protein expression patterns [14]. Re-analysis of our pre-proteomics data showed that proteins related to organization of the ECM, including collagen types III, VIII, XII, XIV, fibronectin 1 (Fn1), periostin (Postn), and metallopeptidase 2 (MMP2), were significantly upregulated (Fig. 2A). qPCR results confirmed the upregulation of collagen 1a1, collagen 3a1 (Col3a1), and Fn1 in cardiac tissue from ISO-treated NKA$\alpha1^{+/-}$ mice (Fig. 2B–D). Myofibroblast differentiation, characterized by upregulation of α-SMA, represents a pivotal event in cardiac fibrogenesis [17]. Immunostaining results showed markedly increased expression of α-SMA in hearts from NKA$\alpha1^{+/-}$ mice (Fig. 2E,F). These findings suggest that NKAα1 haploinsufficiency leads to aberrant ECM deposition and myofibroblast differentiation.

3.3 NKAα1 Haploinsufficiency Increases Macrophage Accumulation and the Expression of Inflammatory Cytokines in ISO-Challenged Hearts

Analysis of our pre-proteomics data revealed increased levels of monocyte and macrophage-related proteins, including CD14, CD68, macrophage-capping protein (Capg), and Galectin-3 (Fig. 3A). We then further detected immune cell infiltration in heart tissues. There was a significantly increased macrophage infiltration in the hearts of ISO-NKA$\alpha1^{+/-}$ mice. The increased macrophages were predominantly localized to fibrotic areas. No significant changes were observed for neutrophil infiltration. Although the number of T cells infiltrating the heart is lower than that of macrophages, it also exhibited significant variations across groups (Fig. 3B–E). Furthermore, NKAα1 haploinsufficiency increased the levels of IL-6, TNF-α, and IL-1β in the heart under ISO-induced conditions compared to controls (Fig. 3F–H).

3.4 Damaged NKA$\alpha1^{+/-}$ Cardiomyocytes Enhanced Macrophage Activation and Fibroblast Differentiation

Since whole-body NKAα1 haploid knockout mice were used in this research, the increased deposition of ECM proteins and macrophage infiltration might result from the direct effects of ISO on NKAα1 haplo-insufficient fibroblast cells or macrophages. Therefore, we first isolated cardiomyocytes, fibroblasts, and macrophages from WT and NKAα1-deficient heterozygous mice and treated them with ISO. NKAα1 haploinsufficiency had no significant effect on the activation of macrophages or fibroblasts (Fig. 4A–C), but exacerbated cardiomyocyte injury, as evidenced by the release of LDH (Fig. 4D). Subsequently, we investigated whether damaged NKA$\alpha1^{+/-}$ cardiomyocytes influenced macrophage activation or fibroblast differentiation. Macrophages or fibroblasts from WT mice were exposed to the primary cultured cardiomyocytes isolated from WT or NKA$\alpha1^{+/-}$ mice and co-cultured them in MEM medium supplemented with 10 μM ISO. Co-culture of cardiomyocytes with macrophages significantly enhanced cytokine

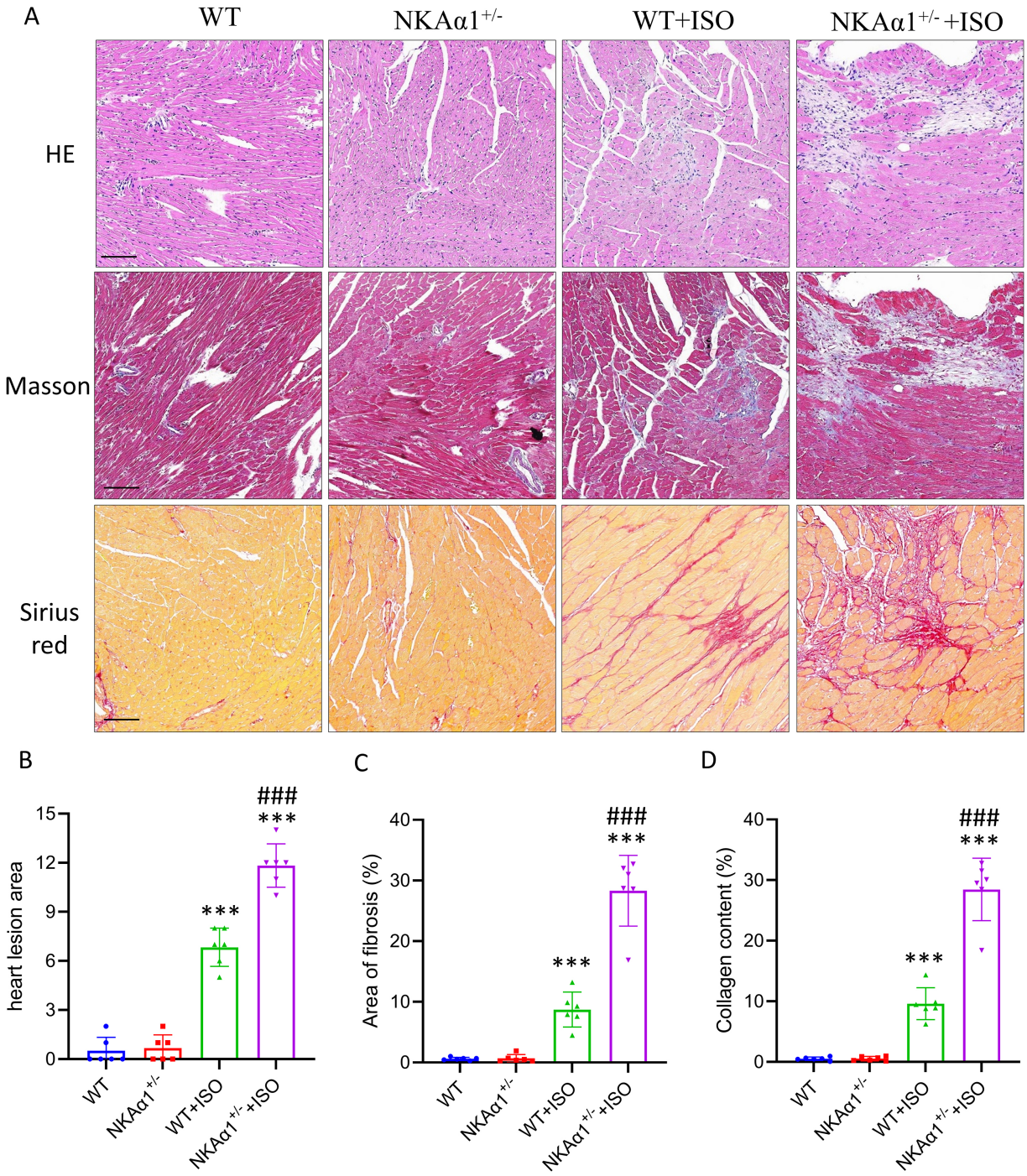

Fig. 1. Na^+, K^+-ATPase (NKA) α1 haploinsufficiency exacerbated isoproterenol (ISO)-induced heart fibrosis. (A) Representative images of hematoxylin and eosin (H&E) staining, Masson staining, and Sirius red staining in the different groups (scale bar = 100 µm). (B) Quantitative assessment of the myocardial lesion area. (C) Quantitative analysis of fibrotic (Masson blue) areas in cardiac sections. (D) Quantitative analysis of collagen (Sirius red) areas in cardiac sections. Data are presented as means ± SD; n = 6. ***$p < 0.001$ for WT+ISO vs wild-type (WT) group and NKA$\alpha1^{+/-}$ + ISO vs NKA$\alpha1^{+/-}$ group; ###$p < 0.001$, vs WT+ISO group.

secretion by the latter cells (Fig. 4E,F). Moreover, co-culture of cardiomyocytes with fibroblasts also increased the expression of α-SMA, an indicator of fibroblast-to-myofibroblast conversion (Fig. 4G). Interestingly, when activated macrophages were co-cultured with fibroblasts, this interaction also increased α-SMA expression (Fig. 4H).

3.5 ERRα Participates in NKAα1 Haploinsufficiency-Induced Cardiomyocyte Death

Subcellular enrichment analysis of our pre-proteomics results revealed significant downregulation of mitochondrial proteins (Fig. 5A). Morphological analysis of mitochondria in heart tissues demonstrated a large number of

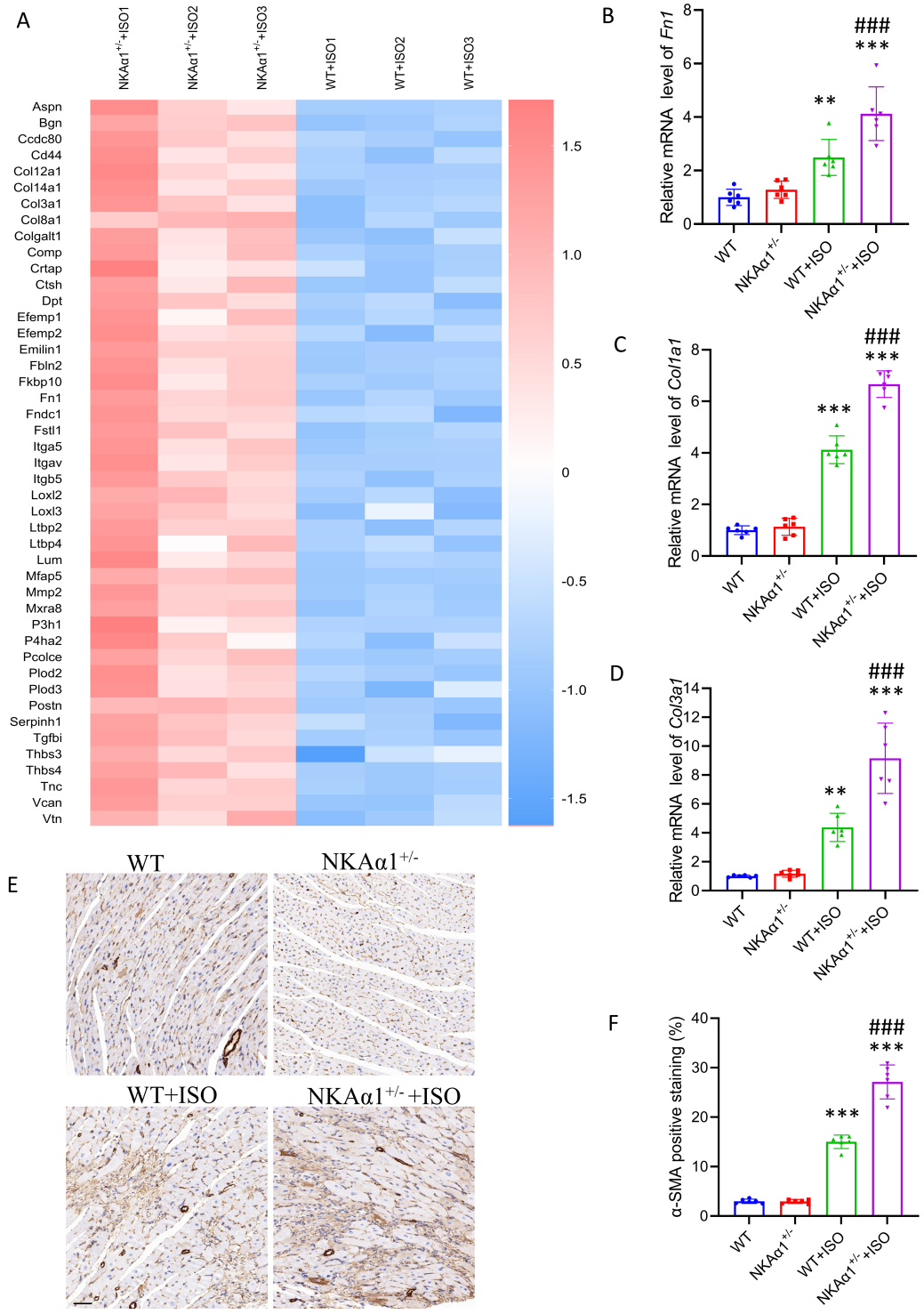

Fig. 2. NKAα1 haploinsufficiency induced the aberrant expression of extracellular matrix (ECM) genes and myofibroblast differentiation. (A) Proteomics analysis of cardiac tissue from ISO-treated WT mice and NKA$\alpha1^{+/-}$ mice. Enrichment map of proteins associated with ECM organization. (B–D) qRT-PCR analysis of Fn1 (B), Col1a1 (C) and Col3a1 (D) expression in cardiac tissues from WT and NKA$\alpha1^{+/-}$ mice treated with saline or ISO. (E) Representative images of α-SMA immunostaining in different groups (scale bar = 50 μm). (F) Quantitative analysis of α-SMA-positive staining areas in cardiac sections. Data are presented as means ± SD; n = 6. $^{**}p < 0.01$, $^{***}p < 0.001$, for WT+ISO vs wild-type (WT) group and NKA$\alpha1^{+/-}$ + ISO vs NKA$\alpha1^{+/-}$ group; $\#\#\#p < 0.001$, vs WT+ISO group.

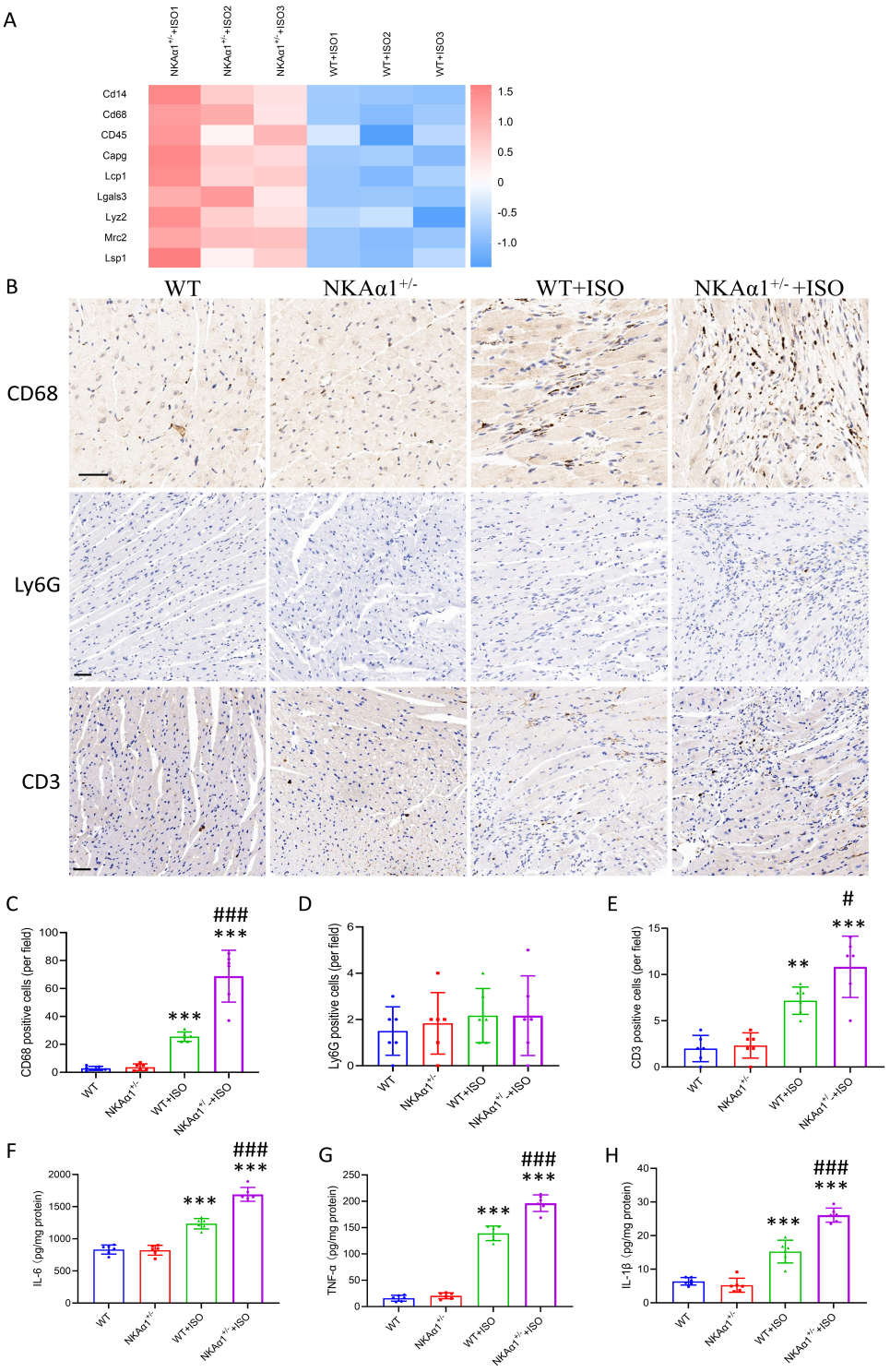

Fig. 3. NKAα1 haploinsufficiency promoted macrophage accumulation and inflammatory factor expression in the ISO-challenged heart. (A) Enrichment map of proteins related to immune cells. (B) Representative images of immunostaining for CD68, LY6G, and CD3 in different groups (scale bar = 50 µm). (C) Quantitative analysis of CD68-positive cells in cardiac sections. (D) Quantitative analysis of Ly6G-positive cells in cardiac sections. (E) Quantitative analysis of CD3-positive cells in cardiac sections. (F–H) ELISA results for interleukin-6 (IL-6), tumor necrosis factor-α (TNF-α), and IL-1β in cardiac tissues from different groups. Data are presented as the mean $\pm$ SD; n = 6. $^{**}p < 0.01$, $^{***}p < 0.001$, for WT+ISO vs wild-type (WT) group and NKA$\alpha1^{+/-}$ + ISO vs NKA$\alpha1^{+/-}$ group; $\#p < 0.05$, $\#\#\#p < 0.001$, vs WT+ISO group.

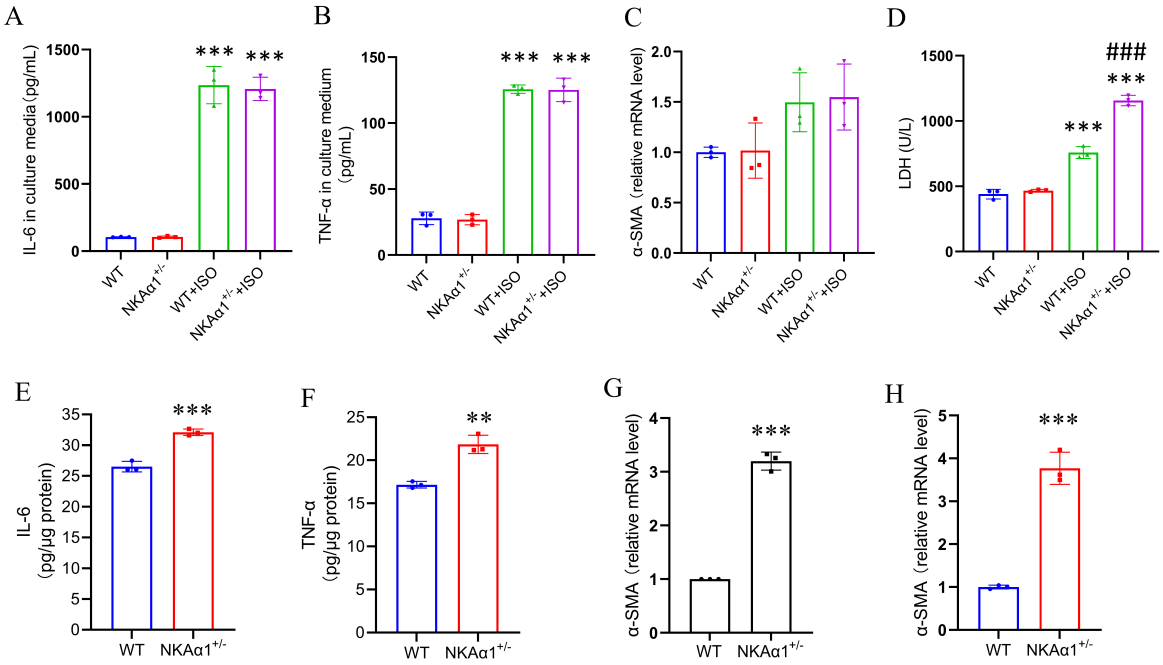

Fig. 4. Impaired NKA$\alpha 1^{+/-}$ cardiomyocytes enhanced macrophages activation and fibroblasts differentiation. (A,B) ELISA results for IL-6 and TNF-α in the culture media of macrophages challenged with ISO or vehicle control. (C) qRT-PCR analysis of α-SMA expression in fibroblasts challenged with ISO or vehicle control. (D) Lactate dehydrogenase (LDH) activity in the culture media of cardiomyocytes challenged with ISO or vehicle control. (E,F) ELISA results for IL-6 and TNF-α in normal macrophages co-cultured with different cardiomyocytes under ISO-challenged conditions. (G) qRT-PCR analysis of α-SMA expression in normal fibroblasts co-cultured with different cardiomyocytes under ISO-challenged conditions. (H) qRT-PCR analysis of α-SMA expression in normal fibroblasts co-cultured with macrophages activated by co-culturing with different cardiomyocytes. Data are presented as the mean $\pm$ SEM; n = 3. $^{**}p < 0.01$, $^{***}p < 0.001$, for: (A–D) WT+ISO vs WT and NKA$\alpha 1^{+/-}$+ISO vs NKA$\alpha 1^{+/-}$ and (E–H) NKA$\alpha 1^{+/-}$ vs WT; $^{\#\#\#}p < 0.001$, vs WT+ISO group.

abnormal mitochondria in the hearts of ISO-NKA$\alpha 1^{+/-}$ mice, characterized by uneven size, disordered arrangement, unclear structure, and disrupted cristae (Fig. 5B). ERRα regulates a large number of genes involved in mitochondrial function [18]. Reanalysis of our pre-proteomics data revealed that ERRα was downregulated in ISO-challenged NKA$\alpha 1^{+/-}$ mice (Fig. 5C). This finding was confirmed by Western blotting (Fig. 5D). SLU-PP-332 is an ERR agonist that has the highest potency for ERRα. Treatment with SLU-PP-332 partially alleviated ISO-induced cell damage in NKA$\alpha 1^{+/-}$ cardiomyocytes (Fig. 5E). It has been reported that ISO induces macrophage infiltration into the heart in an IL-18-dependent manner [19]. ERRα agonists SLU-PP-332 also reduced the release of IL-18 from NKA$\alpha 1^{+/-}$ cardiomyocytes under ISO conditions (Fig. 5F).

3.6 Treatment With NKAα1 DR-Region Antibody Alleviates Macrophage Infiltration and Heart Fibrosis

The DR region (^{897}DVEDSYGQQWTYEQR^{911}) of NKAα1 has been identified as an activation site for NKA [20]. Our group and others reported that DR-region-specific antibodies enhance the activity and level of membrane expression of NKAα1 [15,21]. We subsequently evaluated the effects of DRm217, a specific DR-region monoclonal antibody, on ISO-treated mice. Histopathological analyses revealed that DRm217 attenuated heart lesions, fibrosis, and macrophage accumulation under ISO-challenged conditions (Fig. 6A–D). The levels of inflammatory cytokines, including IL-6, TNF-α, and IL-1β, were also downregulated by DRm217 treatment under ISO-insulted conditions (Fig. 6E–G).

4. Discussion

NKA is a multi-subunit protein complex contains three essential components: α-catalytic subunit, β-regulatory subunit, and γ-modulatory subunit. Cardiac tissue expresses abundant NKA, which plays a critical role in maintaining Na^+ and Ca^{2+} ion gradients, generating action potentials, regulating cell volume, and promoting cell survival [22]. Dysregulation or deficiency of NKA has been observed in various heart diseases, such as acute myocardial infarction, hypertension, and heart failure [12,23,24], indicating its critical contribution to the advancement of cardiovascular pathologies. NKA is closely associated with fibrosis. Cardiotonic steroids (CTS), a class of NKA ligands and inhibitors, have been reported to stimulate fibrob-

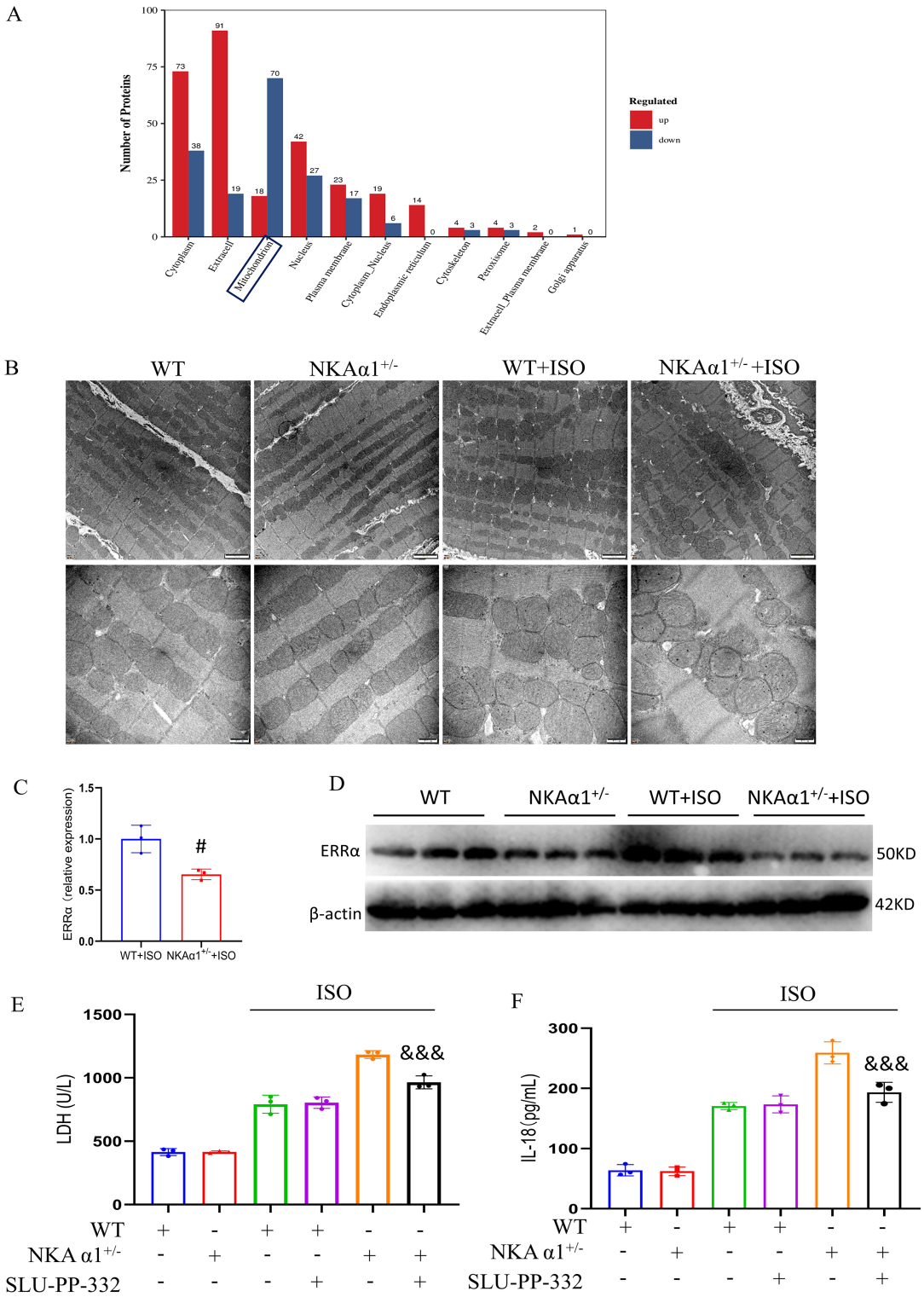

Fig. 5. NKAα1 regulated mitochondria-related myocardial cell injury under ISO-challenged conditions. (A) Subcellular enrichment analysis of differential proteins from proteomics results. (B) Mitochondrial morphology observed by transmission electron microscope (upper panel scale bar, 2 μm; lower panel scale bar, 500 nm). (C) ERRα expression level determined from proteomics results. (D) Western blotting analysis of ERRα in cardiac tissues. (E) LDH content in the culture media of cardiomyocytes treated under different conditions. (F) IL-18 expression in cardiomyocytes treated under different conditions. Data are presented as the mean ± SEM; n = 3. #$p < 0.05$, vs WT+ISO group; &&&, $p < 0.001$, vs NKA$\alpha1^{+/-}$+ISO group.

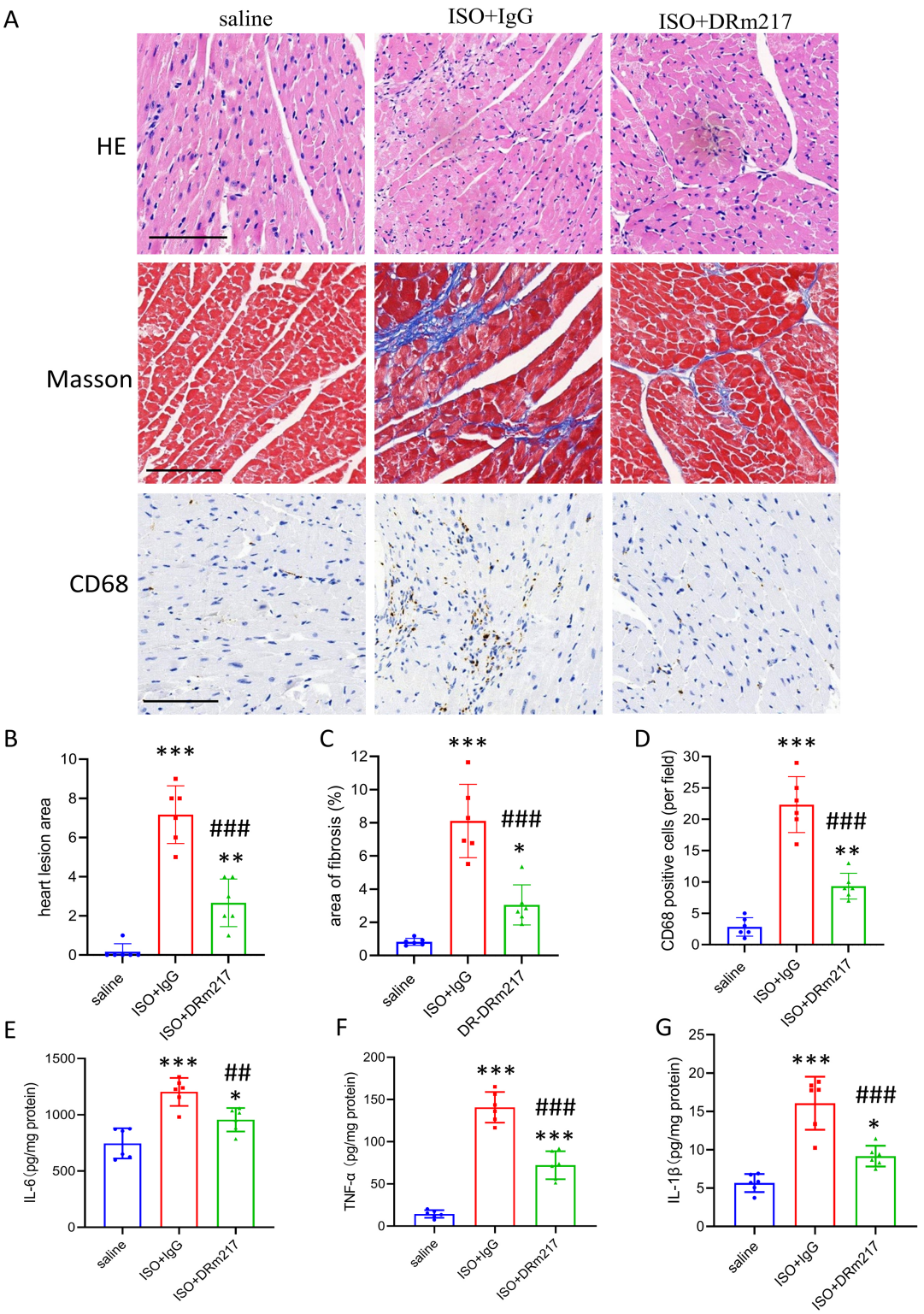

Fig. 6. DRm217 treatment mitigates ISO-induced fibrosis and macrophage activation under ISO-challenged condition. (A) Representative images of H&E, Masson staining, and CD68 immunostaining in different groups (scale bar, 100 μm). (B) Quantitative analysis of the myocardial lesion area. (C) Quantitative analysis of fibrotic (Masson blue) areas in cardiac sections. (D) Quantitative analysis of CD68-positive cells in cardiac sections. (E–G) ELISA results for IL-6, TNF-α, and IL-1β in cardiac tissues from different groups. n = 6. Data are presented as the mean ± SD; *$p < 0.05$, **$p < 0.01$, ***$p < 0.001$, vs saline group; ##$p < 0.01$, ###$p < 0.001$, vs ISO+IgG group.

last collagen production and induce heart or kidney fibrosis [13,25]. Activation of the NKA/Src signaling pathway can initiate miR-29b-3p dysregulation and cardiac fibrogenesis [26]. Furthermore, knockdown of the NKAβ1 subunit in A549 cells resulted in elevated expression of profibrotic factors [27]. However, the relationship between inflammation and NKA-related tissue fibrosis is still unclear. In the present study, we demonstrated that NKAα1 haploinsufficiency exacerbates ISO-induced cardiac lesions, fibrosis, and inflammation. Ventricular tissue from heart failure and dilated cardiomyopathy patients exhibits reduced expression of NKAα1 subunits [12,28]. There have also been reports of elevated plasma catecholamine levels in patients with heart failure [29]. Perhaps the interaction between these two factors may promote heart fibrosis and dysfunction. The current study also found that DRm217, a proven activator of NKA, prevents ISO-induced cardiac lesions, fibrosis, and inflammation under ISO-challenged conditions. These results suggest that regulation of NKA can influence heart fibrosis.

Inflammation serves as a critical driver of maladaptive cardiac remodeling following heart injury [30]. The molecular and cellular mechanisms that underlies inflammatory responses vary across different cardiac diseases [31]. In various models of cardiac disease, heterogeneous inflammatory cells infiltrate to the heart. For example, significant infiltration of neutrophils and inflammatory monocytes occurs in infarcted myocardium [32]. The present study revealed that macrophages are the most abundant infiltrating cell type in the myocardium upon ISO stimulation, consistent with a prior report [20]. NKAα1 exacerbated macrophage infiltration and the expression of inflammatory factors in mouse hearts. Notably, infiltrated macrophages and activated myofibroblasts accumulated mostly in the cardiac lesion area, as evidenced by the results of CD68 and α-SMA immunohistochemical staining. This prompted us to investigate whether the activation of macrophages and fibroblasts was a direct consequence of NKAα1 deficiency under ISO-treated conditions. We treated macrophages and fibroblasts isolated from WT and NKA$\alpha1^{+/-}$ mice with ISO. Our findings indicated that NKAα1 deficiency does not directly activate macrophages or fibroblasts under ISO conditions. However, NKAα1 deficiency accelerated cardiomyocyte death in response to ISO insult. Cell-to-cell communication represents a fundamental characteristic of adult complex organs. Interactions between different cardiac cell types play a crucial role in cardiac fibrotic pathogenesis [33]. Co-culture of NKA$\alpha1^{+/-}$ cardiomyocytes with macrophages increased the secretion of cytokines by the latter cells. Furthermore, the activated macrophages promoted differentiation of fibroblasts. Cells exchange information using chemical, electrical, and mechanical signals, which travel either via direct contact or through the secretion of local mediators like cytokines and growth factors [34]. Through intercellular cross-talk, it appears that damaged NKA$\alpha1^{+/-}$ cardiomyocytes can induce harmful inflammatory responses and thus exacerbate cardiac fibrosis.

Previous studies have demonstrated that suppression of NKAα1 increases the susceptibility of cells to stress-induced death [35,36]. This observation was further substantiated by the experimental results of the present study. Our proteomics analysis revealed that NKAα1 deficiency under ISO-challenged conditions significantly reduced the expression of mitochondrial proteins. Ultrastructural analysis of mitochondrial morphology further confirmed that NKAα1 deficiency markedly accelerated mitochondrial injury in myocardial cells under stress conditions. ERRα is a well-established transcription factor that plays a pivotal role in regulating cellular metabolism and mitochondrial function [37]. Our proteomics and Western blot results showed that ERRα was downregulated in ISO-challenged NKA$\alpha1^{+/-}$ mice. Furthermore, cellular experiments showed that ERRα agonists partially alleviated ISO-induced cell damage in NKA$\alpha1^{+/-}$ cardiomyocytes. It was previously reported that ISO-induced macrophage activation in the heart occurs in an IL-18-dependent manner [20]. ERRα agonists also reduced IL-18 expression in ISO-insulted NKA$\alpha1^{+/-}$ cardiomyocytes. These results suggest that low ERRα expression contributes to the increased susceptibility of NKA$\alpha1^{+/-}$ cardiomyocytes to ISO-induced damage, as well as to the increased release of inflammatory factors. Pan Z *et al*. [38] previously showed that the EGFR/Src pathway regulates ERRα expression. Other reports also indicate that microRNAs, such as miR-135a and miR-137, can modulate ERRα expression [39,40]. Whether NKA signaling pathways are linked to ERRα expression warrants further investigation.

Immune cell infiltration is a significant driver of cardiac fibrosis. Diverse immune populations, including macrophages, T lymphocytes, monocytes, and neutrophils, infiltrate cardiac tissue and participate in injury repair and structural remodeling processes [41]. Concurrently, mitochondrial dysfunction, manifested through impaired metabolism, reduced energy production, elevated mitochondrial reactive oxygen species (mtROS), and disrupted calcium homeostasis, also plays a pivotal role in cardiac pathogenesis [42,43]. Emerging evidence strongly supports an interconnection between immune dysregulation and mitochondrial impairment [44]. On one hand, leaked mitochondrial components, such as mtDNA or mtRNA, can activate inflammatory pathways like cGAS-STING and TLR2/4 [45]. Furthermore, abnormal metabolites and an altered myocardial microenvironment (e.g., lactate accumulation and decreased pH) resulting from mitochondrial dysfunction can drive metabolic reprogramming in immune cells such as macrophages and T lymphocytes [46]. This reprogramming promotes the secretion of pro-inflammatory cytokines, such as IL-6, IL-1β, and TNF-α, thereby triggering inflammatory cascades. On the other hand, inflam-

matory cytokines like TNF-α or IL-1β facilitate mitochondrial permeability transition pore (mPTP) opening, induce mtDNA damage, and disrupt energy metabolism [47]. Although therapeutic strategies targeting inflammatory mediators show promise for cardiac remodeling, clinical trials of specific chemokines/cytokines have achieved limited success [48]. Interventions directly targeting mitochondria are also increasingly recognized as compelling therapeutic strategies for heart disease [49]. In our study, ISO-challenged mice exhibited concurrent mitochondrial impairment and heightened inflammation, effects exacerbated by NKAα1 deficiency. Given the interplay between mitochondrial damage and inflammatory responses, dual-targeted therapies may synergistically prevent myocardial fibrosis.

Postmortem analyses of human failing hearts show ~40% reductions in NKA expression/activity [12]. We previously demonstrated that NKAα1 deficiency under ISO stimulation enhances glycolysis while suppressing TCA cycle activity and oxidative phosphorylation (OXPHOS) [14]. Here, we observed mitochondrial swelling, ultrastructural abnormalities, and increased macrophage infiltration in ISO-treated NKA$\alpha1^{+/-}$ hearts. We highly suspect that injured NKA$\alpha1^{+/-}$ cardiomyocytes release mitochondrial components and metabolites that activate infiltrating immune cells. Li *et al*. [44] linked mitochondrial genes (FBXO7, PGS1) to immune infiltration in septic cardiomyopathy. Our work identifies ERRα as a critical regulator of NKA$\alpha1^{+/-}$ cardiomyocyte injury and inflammatory factor release, suggesting its potential role in immune cell recruitment during ISO-induced cardiomyopathy in NKA deficiency condition. DRm217-mediated NKA activation protected against ISO-induced cardiac lesions, fibrosis, and inflammation. Some studies suggest that enhanced protein degradation serves as the primary mechanism underlying NKAα1 reduction [50,51]. Therefore, inhibiting NKA degradation represents another promising therapeutic approach for preventing cardiac fibrosis.

However, our study has certain limitations. First, we used whole-body NKAα1 haploid knockout mice *in vivo*; these findings should be further validated using cardiomyocyte-specific NKA$\alpha1^{+/-}$ haploid knockout mice to eliminate interference from other factors. Second, although reduced ERRα expression correlated with ISO-induced NKA$\alpha1^{+/-}$ cardiomyocytes injury, the mechanism linking NKA deficiency to ERRα downregulation and the precise role of in ERRα mitochondrial damage require further investigation. Third, it remains to be determined whether macrophage cytokine secretion is triggered by mitochondrial debris or metabolic byproducts from injured NKA$\alpha1^{+/-}$ cardiomyocytes.

5. Conclusion

In summary, our findings demonstrated that NKAα1 haploinsufficiency exacerbated ISO-induced cardiomyocyte death, cardiac lesions, fibrosis, macrophage infiltration, and inflammatory cytokine production. NKA deficiency intensified cardiac fibrosis by increasing ERRα-dependent cardiomyocyte death and facilitating intercellular cross-talk between damaged NKA$\alpha1^{+/-}$ cardiomyocytes, macrophages, and fibroblasts.

Availability of Data and Materials

The datasets used and/or analyzed during the current study are available from the corresponding author upon reasonable request.

Author Contributions

XY, TingL, and HL contributed to the study conception and design. TLei, TLiu, and YL performed the experiments and data acquisition. YL, YZ, RW, and XT established the animal model and and collected experimental data. XY, and HL supervised the project supervised the project, analyzed/interpreted data, draft and critically revised the manuscript. All authors contributed to editorial changes in the manuscript. All authors read and approved the final manuscript. All authors have participated sufficiently in the work and agreed to be accountable for all aspects of the work.

Ethics Approval and Consent to Participate

All animals used in this study were approved by the Animal Care and Use Committee of Xi'an Jiaotong University (Ethics numbers: IAUC/765/2019, #19765). All animal procedures were performed according to the guidelines laid down by the National Health and Medical Research Council of China.

Acknowledgment

Not applicable.

Funding

This work was funded by the National Natural Science Foundation of China (No. 81970220) and Research Incubation Fund of Xi'an People's Hospital (Xi'an Fourth Hospital) (No. ZD-16).

Conflict of Interest

The authors declare no conflict of interest.

References

[1] Ravassa S, López B, Treibel TA, San José G, Losada-Fuentenebro B, Tapia L, *et al*. Cardiac Fibrosis in heart failure: Focus on non-invasive diagnosis and emerging therapeutic strategies. Molecular Aspects of Medicine. 2023; 93: 101194. https://doi.org/10.1016/j.mam.2023.101194.

[2] González A, Schelbert EB, Díez J, Butler J. Myocardial Interstitial Fibrosis in Heart Failure: Biological and Translational Perspectives. Journal of the American College of Cardiology. 2018; 71: 1696–1706. https://doi.org/10.1016/j.jacc.2018.02.021.

[3] Liu M, López de Juan Abad B, Cheng K. Cardiac fibrosis: Myofibroblast-mediated pathological regulation and drug delivery strategies. Advanced Drug Delivery Reviews. 2021; 173: 504–519. https://doi.org/10.1016/j.addr.2021.03.021.

[4] Paulus WJ, Zile MR. From Systemic Inflammation to Myocardial Fibrosis: The Heart Failure With Preserved Ejection Fraction Paradigm Revisited. Circulation Research. 2021; 128: 1451–1467. https://doi.org/10.1161/CIRCRESAHA.121.318159.

[5] Hulsmans M, Sager HB, Roh JD, Valero-Muñoz M, Houstis NE, Iwamoto Y, *et al*. Cardiac macrophages promote diastolic dysfunction. The Journal of Experimental Medicine. 2018; 215: 423–440. https://doi.org/10.1084/jem.20171274.

[6] Nevers T, Salvador AM, Velazquez F, Ngwenyama N, Carrillo-Salinas FJ, Aronovitz M, *et al*. Th1 effector T cells selectively orchestrate cardiac fibrosis in nonischemic heart failure. The Journal of Experimental Medicine. 2017; 214: 3311–3329. https://doi.org/10.1084/jem.20161791.

[7] Hilgendorf I, Frantz S, Frangogiannis NG. Repair of the Infarcted Heart: Cellular Effectors, Molecular Mechanisms and Therapeutic Opportunities. Circulation Research. 2024; 134: 1718–1751. https://doi.org/10.1161/CIRCRESAHA.124.323658.

[8] Yan X, Xun M, Dou X, Wu L, Zhang F, Zheng J. Activation of Na^+-K^+-ATPase with DRm217 attenuates oxidative stress-induced myocardial cell injury via closing Na^+-K^+-ATPase/Src/Ros amplifier. Apoptosis: an International Journal on Programmed Cell Death. 2017; 22: 531–543. https://doi.org/10.1007/s10495-016-1342-2.

[9] Fedosova NU, Habeck M, Nissen P. Structure and Function of Na,K-ATPase-The Sodium-Potassium Pump. Comprehensive Physiology. 2021; 12: 2659–2679. https://doi.org/10.1002/cphy.c200018.

[10] Huang S, Dong W, Lin X, Xu K, Li K, Xiong S, *et al*. Disruption of the Na^+/K^+-ATPase-purinergic P2X7 receptor complex in microglia promotes stress-induced anxiety. Immunity. 2024; 57: 495–512.e11. https://doi.org/10.1016/j.immuni.2024.01.018.

[11] Clausen MV, Hilbers F, Poulsen H. The Structure and Function of the Na,K-ATPase Isoforms in Health and Disease. Frontiers in Physiology. 2017; 8: 371. https://doi.org/10.3389/fphys.2017.00371.

[12] Schwinger RHG, Bundgaard H, Müller-Ehmsen J, Kjeldsen K. The Na, K-ATPase in the failing human heart. Cardiovascular Research. 2003; 57: 913–920. https://doi.org/10.1016/s0008-6363(02)00767-8.

[13] Elkareh J, Kennedy DJ, Yashaswi B, Vetteth S, Shidyak A, Kim EGR, *et al*. Marinobufagenin stimulates fibroblast collagen production and causes fibrosis in experimental uremic cardiomyopathy. Hypertension (Dallas, Tex.: 1979). 2007; 49: 215–224. https://doi.org/10.1161/01.HYP.0000252409.36927.05.

[14] Yan X, Li M, Lan P, Xun M, Zhang Y, Shi J, *et al*. Regulation of Na+-K+-ATPase leads to disturbances of isoproterenol-induced cardiac dysfunction via interference of Ca2+-dependent cardiac metabolism. Clinical Science (London, England: 1979). 2024; 138: 23–42. https://doi.org/10.1042/CS20231039.

[15] Yan X, Xun M, Li J, Wu L, Dou X, Zheng J. Activation of Na+/K+-ATPase attenuates high glucose-induced H9c2 cell apoptosis via suppressing ROS accumulation and MAPKs activities by DRm217. Acta Biochimica et Biophysica Sinica. 2016; 48: 883–893. https://doi.org/10.1093/abbs/gmw079.

[16] Qian J, Wang Q, Xu J, Liang S, Zheng Q, Guo X, *et al*. Macrophage OTUD1-CARD9 axis drives isoproterenol-induced inflammatory heart remodelling. Clinical and Translational Medicine. 2024; 14: e1790. https://doi.org/10.1002/ctm2.1790.

[17] Tarbit E, Singh I, Peart JN, Rose'Meyer RB. Biomarkers for the identification of cardiac fibroblast and myofibroblast cells. Heart Failure Reviews. 2019; 24: 1–15. https://doi.org/10.1007/s10741-018-9720-1.

[18] Li M, Yu Y, Xue K, Li J, Son G, Wang J, *et al*. Genistein mitigates senescence of bone marrow mesenchymal stem cells via ERRα-mediated mitochondrial biogenesis and mitophagy in ovariectomized rats. Redox Biology. 2023; 61: 102649. https://doi.org/10.1016/j.redox.2023.102649.

[19] Xiao H, Li H, Wang JJ, Zhang JS, Shen J, An XB, *et al*. IL-18 cleavage triggers cardiac inflammation and fibrosis upon β-adrenergic insult. European Heart Journal. 2018; 39: 60–69. https://doi.org/10.1093/eurheartj/ehx261.

[20] Xu KY. Activation of (Na+ + K+)-ATPase. Biochemical and Biophysical Research Communications. 2005; 338: 1669–1677. https://doi.org/10.1016/j.bbrc.2005.10.067.

[21] Cao L, Xiong S, Wu Z, Ding L, Zhou Y, Sun H, *et al*. Anti-Na^+/K^+-ATPase immunotherapy ameliorates α-synuclein pathology through activation of Na^+/K^+-ATPase α1-dependent autophagy. Science Advances. 2021; 7: eabc5062. https://doi.org/10.1126/sciadv.abc5062.

[22] Leng B, Deng L, Tan J, Lee WT, Cao CR, Wang ZP, *et al*. Targeting the Na^+/K^+ ATPase DR-region with DR-Ab improves doxorubicin-induced cardiotoxicity. Free Radical Biology & Medicine. 2023; 204: 38–53. https://doi.org/10.1016/j.freeradbiomed.2023.04.008.

[23] Jovanovic A, Obradovic M, Milovanovic ES, Stewart AJ, Pitt SJ, Alavantic D, *et al*. Changes in cardiac Na^+/K^+-ATPase expression and activity in female rats fed a high-fat diet. Molecular and Cellular Biochemistry. 2017; 436: 49–58. https://doi.org/10.1007/s11010-017-3077-y.

[24] Guo HC, Guo F, Zhang LN, Zhang R, Chen Q, Li JX, *et al*. Enhancement of Na/K pump activity by chronic intermittent hypobaric hypoxia protected against reperfusion injury. American Journal of Physiology. Heart and Circulatory Physiology. 2011; 300: H2280–H2287. https://doi.org/10.1152/ajpheart.01164.2010.

[25] Kennedy DJ, Khalaf FK, Sheehy B, Weber ME, Agatisa-Boyle B, Conic J, *et al*. Telocinobufagin, a Novel Cardiotonic Steroid, Promotes Renal Fibrosis via Na^+/K^+-ATPase Profibrotic Signaling Pathways. International Journal of Molecular Sciences. 2018; 19: 2566. https://doi.org/10.3390/ijms19092566.

[26] Drummond CA, Fan X, Haller ST, Kennedy DJ, Liu J, Tian J. Na/K-ATPase signaling mediates miR-29b-3p regulation and cardiac fibrosis formation in mice with chronic kidney disease. PloS One. 2018; 13: e0197688. https://doi.org/10.1371/journal.pone.0197688.

[27] Li B, Huang X, Xu X, Ning W, Dai H, Wang C. The profibrotic effect of downregulated Na,K ATPase β1 subunit in alveolar epithelial cells during lung fibrosis. International Journal of Molecular Medicine. 2019; 44: 273–280. https://doi.org/10.3892/ijmm.2019.4201.

[28] Gao Y, Silva LND, Hurley JD, Fan X, Pierre SV, Sodhi K, *et al*. Gene module regulation in dilated cardiomyopathy and the role of Na/K-ATPase. PloS One. 2022; 17: e0272117. https://doi.org/10.1371/journal.pone.0272117.

[29] Packer M. Beta-adrenergic blockade in chronic heart failure: principles, progress, and practice. Progress in Cardiovascular Diseases. 1998; 41: 39–52. https://doi.org/10.1016/s0033-0620(98)80030-3.

[30] Kawaguchi M, Takahashi M, Hata T, Kashima Y, Usui F, Morimoto H, *et al*. Inflammasome activation of cardiac fibroblasts is essential for myocardial ischemia/reperfusion injury. Circulation. 2011; 123: 594–604. https://doi.org/10.1161/CIRCULATIONAHA.110.982777.

[31] Kologrivova I, Shtatolkina M, Suslova T, Ryabov V. Cells of the Immune System in Cardiac Remodeling: Main Players in Resolution of Inflammation and Repair After Myocardial Infarction. Frontiers in Immunology. 2021; 12: 664457. https:

//doi.org/10.3389/fimmu.2021.664457.
[32] Murtha LA, Schuliga MJ, Mabotuwana NS, Hardy SA, Waters DW, Burgess JK, *et al*. The Processes and Mechanisms of Cardiac and Pulmonary Fibrosis. Frontiers in Physiology. 2017; 8: 777. https://doi.org/10.3389/fphys.2017.00777.
[33] Li W, Lou X, Zha Y, Qin Y, Zha J, Hong L, *et al*. Single-cell RNA-seq of heart reveals intercellular communication drivers of myocardial fibrosis in diabetic cardiomyopathy. eLife. 2023; 12: e80479. https://doi.org/10.7554/eLife.80479.
[34] Ramilowski JA, Goldberg T, Harshbarger J, Kloppmann E, Lizio M, Satagopam VP, *et al*. A draft network of ligand-receptor-mediated multicellular signalling in human. Nature Communications. 2015; 6: 7866. https://doi.org/10.1038/ncomms8866.
[35] Guan H, Lin H, Wang X, Xu Y, Zheng Y, Zhou X, *et al*. Autophagy-dependent Na^+-K^+-ATPase signalling and abnormal urate reabsorption in hyperuricaemia-induced renal tubular injury. European Journal of Pharmacology. 2022; 932: 175237. https://doi.org/10.1016/j.ejphar.2022.175237.
[36] Lan YL, Wang X, Lou JC, Xing JS, Yu ZL, Wang H, *et al*. Bufalin inhibits glioblastoma growth by promoting proteasomal degradation of the Na^+/K^+-ATPase α1 subunit. Biomedicine & Pharmacotherapy = Biomedecine & Pharmacotherapie. 2018; 103: 204–215. https://doi.org/10.1016/j.biopha.2018.04.030.
[37] Eichner LJ, Giguère V. Estrogen related receptors (ERRs): a new dawn in transcriptional control of mitochondrial gene networks. Mitochondrion. 2011; 11: 544–552. https://doi.org/10.1016/j.mito.2011.03.121.
[38] Pan Z, Wang K, Wang X, Jia Z, Yang Y, Duan Y, *et al*. Cholesterol promotes EGFR-TKIs resistance in NSCLC by inducing EGFR/Src/Erk/SP1 signaling-mediated ERRα reexpression. Molecular Cancer. 2022; 21: 77. https://doi.org/10.1186/s12943-022-01547-3.
[39] Zhao Y, Li Y, Lou G, Zhao L, Xu Z, Zhang Y, *et al*. MiR-137 targets estrogen-related receptor alpha and impairs the proliferative and migratory capacity of breast cancer cells. PloS One. 2012; 7: e39102. https://doi.org/10.1371/journal.pone.0039102.
[40] Tribollet V, Barenton B, Kroiss A, Vincent S, Zhang L, Forcet C, *et al*. miR-135a Inhibits the Invasion of Cancer Cells via Suppression of ERRα. PloS One. 2016; 11: e0156445. https://doi.org/10.1371/journal.pone.0156445.
[41] Tian Y, Wang Z, Liang F, Wang Y. Identifying Immune Cell Infiltration and Hub Genes During the Myocardial Remodeling Process After Myocardial Infarction. Journal of Inflammation Research. 2023; 16: 2893–2906. https://doi.org/10.2147/JIR.S416914.
[42] Gallo G, Rubattu S, Volpe M. Mitochondrial Dysfunction in Heart Failure: From Pathophysiological Mechanisms to Therapeutic Opportunities. International Journal of Molecular Sciences. 2024; 25: 2667. https://doi.org/10.3390/ijms25052667.
[43] Varghese LN, Katare R. Exploring the Link between Metabolic Remodelling and Reactive Oxygen Species in the Aged and Diseased Heart. Frontiers in Bioscience (Landmark edition). 2024; 29: 249. https://doi.org/10.31083/j.fbl2907249.
[44] Li Y, Yu J, Li R, Zhou H, Chang X. New insights into the role of mitochondrial metabolic dysregulation and immune infiltration in septic cardiomyopathy by integrated bioinformatics analysis and experimental validation. Cellular & Molecular Biology Letters. 2024; 29: 21. https://doi.org/10.1186/s11658-024-00536-2.
[45] Ding W, Chen J, Zhao L, Wu S, Chen X, Chen H. Mitochondrial DNA leakage triggers inflammation in age-related cardiovascular diseases. Frontiers in Cell and Developmental Biology. 2024; 12: 1287447. https://doi.org/10.3389/fcell.2024.1287447.
[46] Hang L, Zhang Y, Zhang Z, Jiang H, Xia L. Metabolism Serves as a Bridge Between Cardiomyocytes and Immune Cells in Cardiovascular Diseases. Cardiovascular Drugs and Therapy. 2025; 39: 661–676. https://doi.org/10.1007/s10557-024-07545-5.
[47] Deo P, Chow SH, Han ML, Speir M, Huang C, Schittenhelm RB, *et al*. Mitochondrial dysfunction caused by outer membrane vesicles from Gram-negative bacteria activates intrinsic apoptosis and inflammation. Nature Microbiology. 2020; 5: 1418–1427. https://doi.org/10.1038/s41564-020-0773-2.
[48] Harding D, Chong MHA, Lahoti N, Bigogno CM, Prema R, Mohiddin SA, *et al*. Dilated cardiomyopathy and chronic cardiac inflammation: Pathogenesis, diagnosis and therapy. Journal of Internal Medicine. 2023; 293: 23–47. https://doi.org/10.1111/joim.13556.
[49] Zhang A, Liu Y, Pan J, Pontanari F, Chia-Hao Chang A, Wang H, *et al*. Delivery of mitochondria confers cardioprotection through mitochondria replenishment and metabolic compliance. Molecular Therapy: the Journal of the American Society of Gene Therapy. 2023; 31: 1468–1479. https://doi.org/10.1016/j.ymthe.2023.02.016.
[50] Zhang J, Li X, Yu H, Larre I, Dube PR, Kennedy DJ, *et al*. Regulation of Na/K-ATPase expression by cholesterol: isoform specificity and the molecular mechanism. American Journal of Physiology. Cell Physiology. 2020; 319: C1107–C1119. https://doi.org/10.1152/ajpcell.00083.2020.
[51] Lecuona E, Sun H, Vohwinkel C, Ciechanover A, Sznajder JI. Ubiquitination participates in the lysosomal degradation of Na,K-ATPase in steady-state conditions. American Journal of Respiratory Cell and Molecular Biology. 2009; 41: 671–679. https://doi.org/10.1165/rcmb.2008-0365OC.